Formation of Dispersive Shock Waves by Merging and Splitting Bose-Einstein Condensates

J. J. Chang and P. Engels*
Washington State University, Department of Physics and Astronomy, Pullman, Washington, D.C. 99164, USA
M. A. Hoefer
National Institute of Standards and Technology, Boulder, Colorado 80305, USA+
(Received 14 March 2008; published 23 October 2008)

The processes of merging and splitting dilute-gas Bose-Einstein condensates are studied in the nonadiabatic, high-density regime. Rich dynamics are found. Depending on the experimental parameters, uniform soliton trains containing more than ten solitons or the formation of a high-density bulge as well as dispersive shock waves are observed experimentally within merged BECs. Our numerical simulations indicate the formation of many vortex rings. In the case of splitting a BEC, the transition from sound-wave formation to dispersive shock-wave formation is studied by use of increasingly stronger splitting barriers. These experiments realize prototypical dispersive shock situations.

DOI: 10.1103/PhysRevLett.101.170404 PACS numbers: 03.75.Kk, 05.45.−a, 47.40.−x, 67.85.De

Dilute-gas Bose-Einstein condensates (BECs) are a powerful environment for the study of nonlinear dynamics. Dispersive shock waves (DSWs) are an example of nonlinear behavior which has generated interest among diverse areas of physics. First studied in water and plasma wave dynamics [1], DSWs have also been investigated in other areas where dispersive hydrodynamic behavior is possible including nonlinear optics [2], electronic liquids [3], and ultracold quantum gases [4–9]. The theoretical foundation for the study of DSWs in BECs is the small dispersion limit of the one-dimensional nonlinear Schrödinger equation (NLS) that was first studied in [10] and later in many works including [4–8]. More generally, the three-dimensional NLS equation with a linear potential and small dispersion (also known as the Gross-Pitaevskii equation) describes an interacting BEC that can give rise to shock dynamics [8]. In this Letter, we investigate dispersive hydrodynamics in BECs via the merging and splitting of condensates in the nonadiabatic, high-density regime. We realize several important prototypical situations which have been discussed in previous theoretical studies [4–8]. After merging two BECs, we can observe many solitons (a soliton train). For low enough atom numbers, the soliton train is uniform, as predicted for a one-dimensional situation [4,11,12]. For higher atom numbers, a high-density bulge emerges, and our numerical simulations suggest that this bulge consists of many vortex rings due to a transverse instability of the soliton train. A precise understanding of the merging dynamics is also essential from a technological point of view. For example, merging processes are fundamental operations in atom interferometers [13,14] and in the creation of a "continuous BEC" [15] where a condensate is continuously replenished by newly condensed atoms. Furthermore, vortex formation during the merging of multiple BECs has been used as a tool to investigate the relative phases between BECs [16]. Splitting a BEC with a repulsive barrier can also lead to DSWs, and we observe a transition from propagating sound waves to DSWs when a sufficiently strong barrier is used. Finally, we find shock dynamics in yet a different setting, namely, when a high-density region in a BEC is suddenly released and allowed to spread into a surrounding background of condensed atoms. Our results complement previous experiments that considered either very narrow initial gaps in a BEC, produced by a stopped-light technique [9,17], or blast pulses in rotating [18] and nonrotating [8] cylindrical geometries.

All our experiments begin with ultracold clouds of ^{87}Rb atoms in the $|F, m_F\rangle = |1, -1\rangle$ hyperfine state. The atoms are magnetically contained in an elongated Ioffe-Pritchard type trap with frequencies $\{\omega_x/(2\pi), \omega_{yz}/(2\pi)\} = \{7, 402\}$ Hz (the x-axis is oriented horizontally). Repulsive and attractive barriers for the atoms are created with dipole lasers that are far detuned from the Rb D-lines at 780 and 795 nm. The dipole laser beams are sent horizontally through the center of the magnetic trap, along the radial (tightly confining) y-direction. In the vertical direction (z-axis), the laser waist is much larger than the radial extent of the BECs. Dynamics are induced in the BEC by rapidly turning a dipole beam on or off. To enlarge the resulting features, we employ a 2 ms long antitrapped expansion before imaging [19]. During this expansion, the aspect ratio of a BEC formed without the presence of a dipole barrier changes from 57 for the trapped BEC to about 3.

In a first set of experiments, the dynamics of merging two BECs in the nonadiabatic, high-density regime are studied. For this, a dipole beam with a wavelength of $\lambda = 660$ nm, a power of 3.48 mW, and waists of $w_x = 27.3$ μm and $w_z = 32.1$ μm is used, creating a repulsive barrier with a height of 490 nK for the atoms. The total atom number for the experiments shown in Figs. 1(a)–1(e) and 1(n) is about 1×10^6 atoms. For a single BEC confined in the

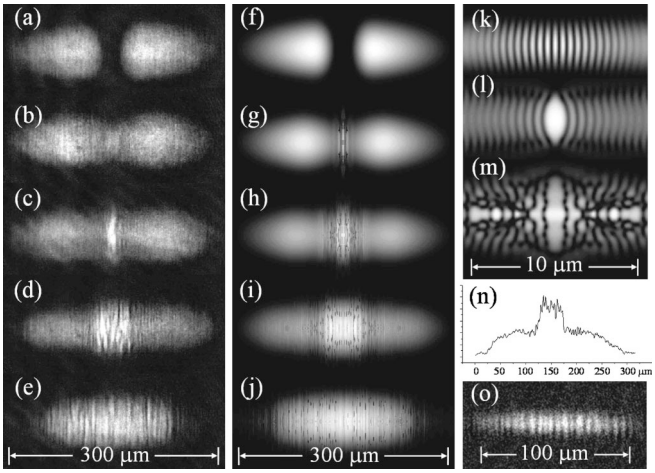

FIG. 1. Left column: experimental antitrapped expansion images of a BEC collision at $t =$ (a) 2 ms, (b) 7 ms, (c) 12 ms, (d) 22 ms, and (e) 57 ms (including the 2 ms antitrapped expansion time). Middle column: numerical simulations at $t =$ (f) 2 ms, (g) 7 ms, (h) 12 ms, (i) 22 ms, and (j) 57 ms. The antitrapped expansion was not simulated; therefore, the vertical scale of (f)–(j) is about $\frac{3}{57}$ the vertical scale of (a)–(e), see also [20]. Right column: (k)–(m) simulations showing zoomed-in density slices of the BEC by the plane $z = 0$ after (k) 5 ms, (l) 6.25 ms, and (m) 7.5 ms. (n) Integrated cross section of (d). (o) Typical uniform soliton train observed for lower atom numbers (experimental image; parameters see text).

magnetic trap, this would imply a chemical potential of $\mu = 224$ nK. Therefore, the presence of the dipole beam leads to two clearly separated BECs [Fig. 1(a)]. The beam is turned on before the atoms are evaporatively cooled to form a BEC. After a BEC has formed on both sides of the barrier and no surrounding thermal cloud is visible, the dipole beam is rapidly turned off within less than 250 ns. We let the dynamics evolve in the magnetic trap for a variable evolution period before starting the expansion imaging. Directly after turning the dipole barrier off, the condensates smoothly expand toward each other [Fig. 1(b)]. This behavior can be described by the well-known dam-breaking problem whereby a sharp density gradient develops into a rarefaction wave (as opposed to a shock wave) when the background density is zero (see, e.g., [8,10]). Shortly after the BECs have collided at the center of the trap, a pronounced bulge of higher atom density forms in the collision plane [Fig. 1(c)]. Very pronounced dark notches are observed to form within the high-density bulge as shown in Fig. 1(d). Subsequently, this density bulge spreads out from the center of the trap [Figs. 1(c)–1(e) and 1(n)], and more notches are formed to fill the extent of the density bulge with an average spacing of roughly 8 to 11 μm. After about 55 ms, the bulge and the notches have spread over the entire extent of the condensate [Fig. 1(e)]. The long lifetime, discrete nature, and large amplitude of the notches suggest that they are nonlinear coherent structures rather than simple sound waves. Our numerical simulations show that a soliton train initially develops and a bulge region is formed where the solitons decay into a large number of vortex rings, see Figs. 1(f)–1(m) and [20]. Experimentally, vortex rings in BECs have been observed in [17,21]. They are difficult to detect unambiguously in our experimental images that are integrated along the line of sight. Fine fringes appear adjacent to the bulge region as can be seen, e.g., in Figs. 1(d) and 1(i). The fine fringes, together with the steepness of the wave fronts delimiting the density bulge region, are indicative of DSWs. The merging process finally results in an axial breathing-mode excitation of the BEC.

The qualitative features of the evolution are fairly independent of most experimental parameters. For example, use of two BECs with an initial total atom number of 2.2×10^6 atoms and a dipole beam with waists of $w_x = 8.5$ μm and $w_z = 32.1$ μm gives qualitatively the same results [see Fig. 2(b)]. However, when the atom number is strongly reduced, we observe a transition in the merging dynamics, both experimentally and numerically, from the generation of a high-density bulge to the generation of a uniform soliton train with no bulge. A typical image of such a soliton train is shown in Fig. 1(o) for 22 000 atoms, a dipole beam power of 150 μW, an evolution time of 27 ms, and an expansion time of 1 ms (see also [20]). The transition can be understood in the following way. A BEC dark soliton is unstable to long transverse wavelength perturbations leading to vortex formation (see, e.g., [9]). As numerical simulations show {Figs. 1(k)–1(m) and [20]}, the pronounced bulge in Figs. 1(c)–1(e) coincides with the existence of vortices. By reducing the nonlinearity in the system, we have effectively lengthened the soliton instability wavelength beyond the radial extent of the BEC; thus, the soliton train remains effectively one-dimensional and stable as in Fig. 1(o) and [20]. A one-dimensional analysis reveals that the soliton train can be interpreted as the result of the interaction of two rarefaction waves generated by two dam-breaking problems [22]. A detailed analysis of this transition is beyond the scope of this work.

In a second set of experiments, we investigate the dynamics of splitting a BEC with a repulsive barrier that is suddenly turned on in the center of the BEC. For very weak barriers that only slightly modify the BEC density, the sudden turn-on leads to the propagation of sound waves [23,24]. Strong barriers, in contrast, lead to DSWs. We first create BECs with 2.2×10^6 atoms in the magnetic trap without the presence of the dipole barrier. Then, a dipole beam with waists of $w_x = 8.5$ μm and $w_z = 32.1$ μm is rapidly turned on and left on for a variable evolution time, after which the antitrapped expansion procedure is started. The rapid turn-on of the dipole beam produces two density peaks that spread out to either side, as shown in Fig. 2(c). The measured propagation speed of these peaks in the central region of the BECs is plotted in Fig. 3 for various powers of the dipole beam [25]. For the lowest powers, the speed is in full agreement with the calculated longitudinal speed of sound, 3.8 mm/s [26]. At these low powers, the density peaks are barely visible in the cloud. For stronger

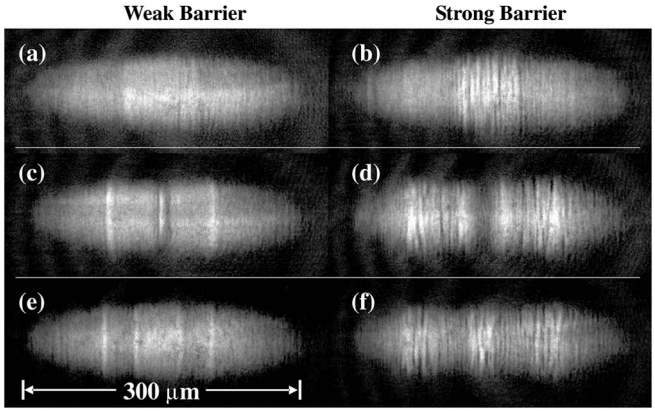

FIG. 2. Dynamics induced by repulsive barrier. (a), (b) Turning a barrier off after forming a BEC in the presence of the barrier. (c), (d) Turning a barrier on after forming a BEC without the presence of the barrier. (e), (f) Pulsing the barrier on for 1.5 ms after the formation of a BEC without the presence of the barrier. (a), (c), (e) Weak barrier, laser power 360 μW. (b), (d), (f) Strong barrier, laser power 1.99 mW. Evolution times before start of imaging procedure: (a), (b) 16 ms, (c), (d) 12 ms, (e), (f) 10 ms.

dipole beams, the propagation speed increases above the speed of sound, and for sufficiently strong beams the obtained images change qualitatively due to dispersive shock formation. For laser powers above approximately 0.6 mW, fine fringes appear in front of the propagating peaks. When the dipole beam exceeds a power of roughly

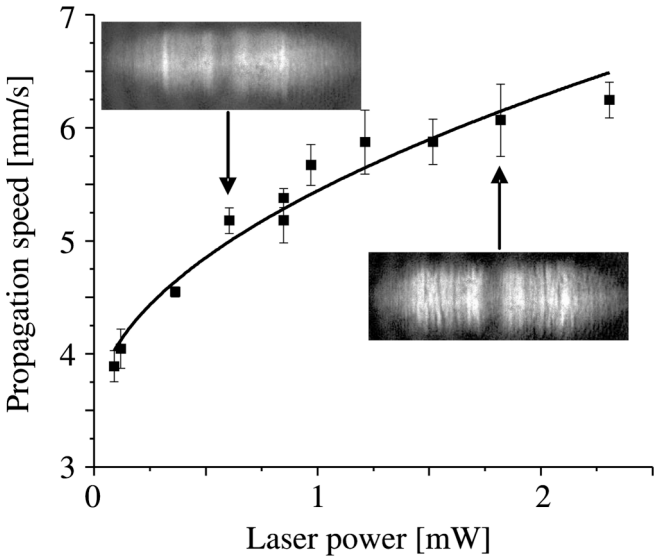

FIG. 3. Speed of wave front propagation through a BEC. After a BEC is formed, a repulsive dipole laser is suddenly turned on. The plot shows the propagation speed of the resulting wave fronts vs the applied laser power. Error bars are taken from fits of distances vs time. The line shows the function $v(P) = a + b\sqrt{P}$ fitted to the data. Insets show two representative images obtained with an evolution time of 12.5 ms and a laser power, respectively, below and above the power at which the wave fronts start breaking into solitons.

1.2 mW, solitons are formed in the region between the two wave fronts, as shown in Fig. 2(d). For an oblate rather than cigar-shaped geometry, related ring-shaped structures have been interpreted in the context of DSWs in [8]. Numerical simulations [20] suggest that this behavior is qualitatively described as follows. Two peaks in the density and outward superfluid velocity are generated by the repulsive dipole beam. These peaks break due to nonlinear steepening [6], causing the generation of two DSWs on the inner and outer edges of each peak. Because of a transverse instability, these quasi-one-dimensional DSWs break up into many vortex rings, leading to interactions. The interaction of DSWs has been studied experimentally in [2,17] and theoretically in [5]. Deriving an analytic expression for the DSW speeds is complicated by the generation of vortex rings and wave interactions. Empirically, the dependence of pulse propagation speed on the dipole laser power is described reasonably well by a square-root dependence, as shown by the fitted curve in Fig. 3.

Our experiments reveal that rapidly switching on a weak dipole barrier merely leads to two density peaks that spread out [Fig. 2(c)], whereas for strong barriers, soliton formation is observed in the wake behind the wave fronts [Fig. 2(d)]. A similar transition also exists for the merging of BECs: If two BECs are initially separated by a strong barrier, soliton dynamics are observed after turning the barrier off, as described in detail above [Figs. 1 and 2(b)]. If, however, the initial dipole barrier is so weak that it merely produces a small density suppression in an initial BEC, a density bulge that does not contain solitons [Fig. 2(a)] appears after the turnoff. Pulsing a barrier on for a short time combines the effects of turning on and turning off a barrier [Figs. 2(e) and 2(f)]; see also [20].

Yet another, different prototypical DSW situation comes about when a local high-density peak in a BEC is suddenly released and is allowed to spread out into a surrounding background of lower density. We can realize this experimentally by replacing the 660 nm dipole laser with an 830 nm laser, leading to an attractive dipole potential. In Figs. 4(a)–4(d), such an attractive dipole beam with a waist of $w_x = 5$ μm and $w_z = 41$ μm and a power of 61 μW is sent through the center of the magnetic trap in the radial direction. Evaporative cooling in the presence of the combined optical and magnetic potential leads to a BEC with a localized high-density peak in its center [Fig. 4(a)]. When the dipole beam is suddenly switched off after the formation of the BEC, the central high-density peak spreads out into the surrounding parts of the BEC. Interestingly, the high-density peak does not remain a single peak but quickly splits into two peaks [Fig. 4(b)] that subsequently travel outward in opposite directions [Figs. 4(c) and 4(d)]. Indeed such splitting is expected from theory [6] and has been observed in nonlinear optics [2]. Following [5], one can show that in the quasi-one-dimensional regime, two counterpropagating DSWs interacting with trailing rarefaction waves are generated in such a situation. For the

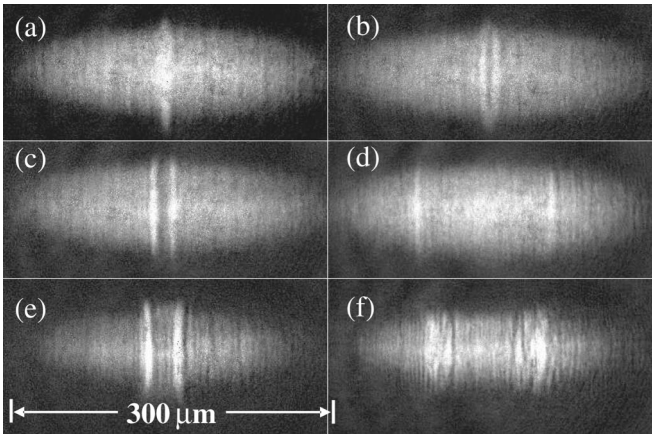

FIG. 4. Dynamics induced by suddenly turning off a local, attractive dipole potential in the center of a BEC. Dipole laser wavelength 830 nm, power 61 μW. Evolution time between turnoff and start of expansion: (a) 0 ms, (b) 0.25 ms, (c) 1 ms, (d) 14 ms. (e), (f) Development of dispersive shock waves when a laser power of 183 μW is used. Evolution time (e) 1 ms, (f) 8 ms.

parameters in Figs. 4(a)–4(d), the measured propagation speed of the two propagating peaks is 4.34 mm/s. When the initial dipole beam power is reduced, the measured speed decreases and approaches the longitudinal speed of sound. When a stronger dipole beam with a power of 183 μW is used, again two peaks form and spread out [Fig. 4(e)], but now DSWs form, marked by solitons in the inner region and strong ripples in the outer regions of the BEC [Fig. 4(f)]; see also [20].

In summary, our experiments realize several prototypical situations for dispersive shock wave formation and demonstrate the transition from sound wave propagation to dispersive shock dynamics as increasingly stronger perturbations are applied. Several aspects of this behavior, such as the splitting of an initial single peak into two (Fig. 4) followed by the formation of dispersive shock waves, are very similar to those observed in nonlinear optics. This demonstrates the generality of our results and showcases the usefulness of BECs in the study of nonlinear wave dynamics.

P. E. acknowledges financial support from NSF under Grant No. PHY-0652976.

Note added.—Recently, two further papers using merging of BECs to create two solitons appeared [27].

*engels@wsu.edu

[1] R. J. Taylor, D. R. Baker, and H. Ikezi, Phys. Rev. Lett. **24**, 206 (1970); A. V. Gurevich and L. P. Pitaevskii, Sov. Phys. JETP **38**, 291 (1974).
[2] See, e.g., W. Wan, S. Jia, and J. W. Fleischer, Nature Phys. **3**, 46 (2007), and references therein.
[3] E. Bettelheim, A. G. Abanov, and P. Wiegmann, Phys. Rev. Lett. **97**, 246401 (2006).
[4] B. Damski, Phys. Rev. A **73**, 043601 (2006).
[5] M. A. Hoefer and M. J. Ablowitz, Physica D (Amsterdam) **236**, 44 (2007).
[6] B. Damski, Phys. Rev. A **69**, 043610 (2004).
[7] A. M. Kamchatnov, A. Gammal, and R. A. Kraenkel, Phys. Rev. A **69**, 063605 (2004).
[8] M. A. Hoefer *et al.*, Phys. Rev. A **74**, 023623 (2006).
[9] Z. Dutton *et al.*, Science **293**, 663 (2001).
[10] A. V. Gurevich and A. L. Krylov, Zh. Eksp. Teor. Fiz. **92**, 1684 (1987); G. A. El *et al.*, Physica D (Amsterdam) **87**, 186 (1995).
[11] W. P. Reinhardt and C. W. Clark, J. Phys. B **30**, L785 (1997).
[12] V. A. Brazhnyi and A. M. Kamchatnov, Phys. Rev. A **68**, 043614 (2003).
[13] C. Lee, E. A. Ostrovskaya, and Y. S. Kivshar, J. Phys. B **40**, 4235 (2007).
[14] See, e.g., G.-B. Jo *et al.*, Phys. Rev. Lett. **98**, 180401 (2007); R. G. Scott, T. E. Judd, and T. M. Fromhold, Phys. Rev. Lett. **100**, 100402 (2008), and references therein.
[15] A. P. Chikkatur *et al.*, Science **296**, 2193 (2002).
[16] D. R. Scherer *et al.*, Phys. Rev. Lett. **98**, 110402 (2007); V. Schweikhard, S. Tung, and E. A. Cornell, Phys. Rev. Lett. **99**, 030401 (2007).
[17] N. S. Ginsberg, J. Brand, and L. V. Hau, Phys. Rev. Lett. **94**, 040403 (2005).
[18] T. P. Simula *et al.*, Phys. Rev. Lett. **94**, 080404 (2005).
[19] H. J. Lewandowski *et al.*, J. Low Temp. Phys. **132**, 309 (2003).
[20] See EPAPS Document No. E-PRLTAO-101-067840 for the numerical simulations. For more information on EPAPS, see E-PRLTAO-101-067840.
[21] B. P. Anderson *et al.*, Phys. Rev. Lett. **86**, 2926 (2001).
[22] M. A. Hoefer, P. Engels, and J. J. Chang, Physica D (Amsterdam) (to be published).
[23] M. R. Andrews *et al.*, Phys. Rev. Lett. **79**, 553 (1997).
[24] J. Joseph *et al.*, Phys. Rev. Lett. **98**, 170401 (2007).
[25] The two density peaks slightly slow down as they travel towards outer edges of the BEC. Therefore, we fit a polynomial of order 2 to the measurements of position vs propagation time, which fits the data very well. We quote the coefficient of the linear term as the central speed of sound. The peak seen in the middle of the BEC in Fig. 2(c) is due to merging dynamics that take place during the antitrapped expansion just prior to imaging (the dipole barrier was off during the 2 ms long antitrapped expansion).
[26] E. Zaremba, Phys. Rev. A **57**, 518 (1998); S. Stringari, Phys. Rev. A **58**, 2385 (1998); G. M. Kavoulakis and C. J. Pethick, Phys. Rev. A **58**, 1563 (1998).
[27] A. Weller *et al.*, arXiv:0803.4352; I. Shomroni *et al.*, arXiv:0805.3263.